

8

Rheology of Gum Rubber and Compound

8.1 Rheometry

Rheology is a study of deformation and flow. In a simplistic way the deformation may be associated with elasticity and the flow with viscosity. Then, rheology is synonymous to viscoelasticity. Indeed, sometimes these terms are used interchangeably. An extensive treatment has already been given for the viscoelastic behaviour of gum rubbers and compounds in Chapter 6 and 7.

The reasons why rheology is selected as a separate chapter is as follows: the capillary rheometer and the rotational rheometer, which had originally been designed for the rheological measurements of liquids have been used for the observation of gum rubber and compound behaviour. The question is what these measurements really mean, because gum rubbers as well as compounds are not liquids but they are in the rubbery state. However, in this chapter, the conventional practice of treating the material as if it were liquid is followed. Not only is the viscosity-shear rate relationship discussed but also the melt fracture, extrudate swell and slip. Shown in Figure 8.1 are ‘flow curves’ of NBR samples, A, B, C, and D at 100 °C [1].

These curves are very much like the ones obtained with thermoplastic melts, exhibiting a non-Newtonian behaviour. The only difference is that with the plastic melt the curves become flatter, decreasing the negative slope with the decreasing shear rate. This suggests that if the lower shear-rate-data were obtained, the extension of the curves of Figure 8.1 would become like those of the thermoplastics.

From this discussion the question arises, of whether or not the flow mechanism is the same for plastic melt and rubber throughout the shear-rate range of non-Newtonian flow. As pointed out with the curve A, the melt fracture occurs at a shear rate higher than that indicated by the arrow. With the other three samples the melt fracture occurred over the entire range of the shear rate. The appearance of the extrudates is depicted in Figure 8.2. Onset of the melt fracture suggests some sort of a discontinuity.

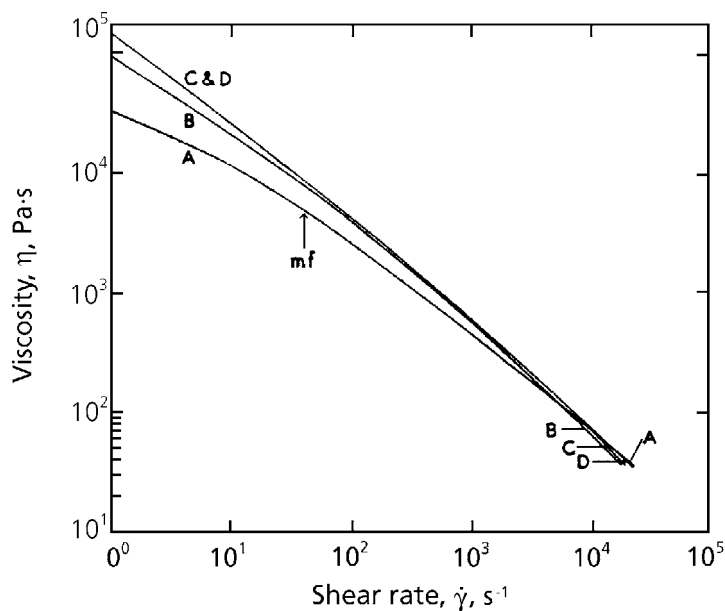


Figure 8.1 Flow curves of Samples A, B, C and D at 100 °C; mf is the onset of melt fracture.

Reprinted from N. Nakajima and E. A. Collins, Polymer Engineering and Science, 1974, 14, 2, 137. Copyright 1974, Society of Plastics Engineering.

This is consistent with the previously described viscoelastic behaviour of gum rubber where there is a transition from the rubbery state to the flow state over a longer time scale. The longer time scale corresponds to the lower shear rate where the material is in the flow state.

With the higher MW rubber the flow-rubber transition occurs at the lower shear rate so that the transition does not appear in Figure 8.1 for samples B, C, and D. When the gum rubbers in the rubbery state are pushed from the barrel of the rheometer into the capillary they break because the large deformation from the barrel to capillary exceeds the breaking strain.

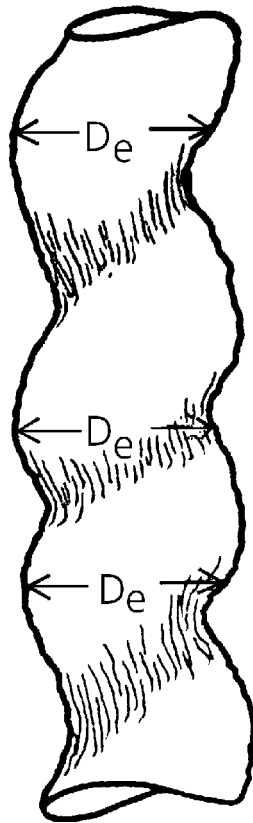


Figure 8.2 Shape of distorted extrudate. D_e is the extrudate diameter.

Reprinted from N. Nakajima and E. A. Collins, Polymer Engineering and Science, 1974, 14, 2, 137. Copyright 1974, Society of Plastics Engineering.

Next the behaviour of the ‘flow’, which is in reality a combination of the fracture and a bulk transport through capillary will be examined.

Figure 8.3 is a plot of pressure (expressed as a force on the piston) against the L/D of the capillary at fixed shear rates.

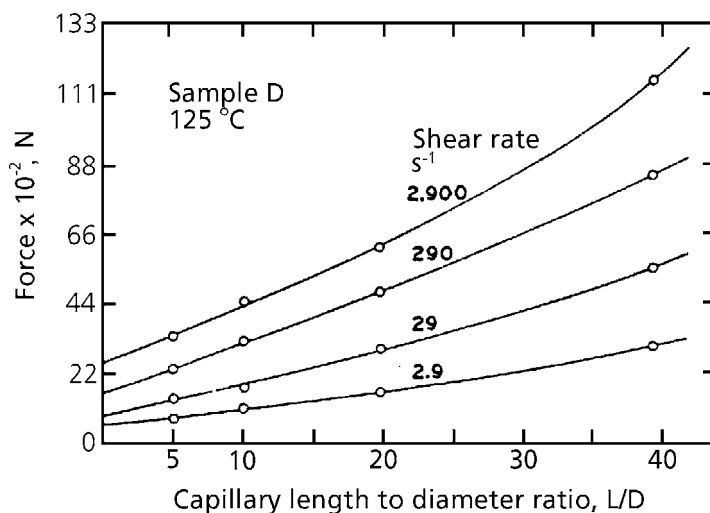


Figure 8.3 Pressure versus capillary L/D at constant shear rate for Sample D at 125°C .

Reprinted from N. Nakajima and E. A. Collins, Polymer Engineering and Science, 1974, 14, 2, 137. Copyright 1974, Society of Plastics Engineering.

These curves look very much like the ones obtained with thermoplastic melts, except that the entrance pressure loss (the force at $L/D = 0$ in the figure), is much larger. With thermoplastic melt, this loss consists of the viscous resistance of flow in the barrel and the elastic energy associated with deformation at the constriction leading into the capillary. With rubbers the energy of break must have a significant contribution.

The behaviour of rubber at the capillary entrance is similar to that in the transient region observed by the rotational rheometer, see Figure 4.6 [2]. The peak of the torque-rise curve is interpreted to be breaking strain and compared to that observed with the tensile stress-strain measurement, see Figure 8.4 [3].

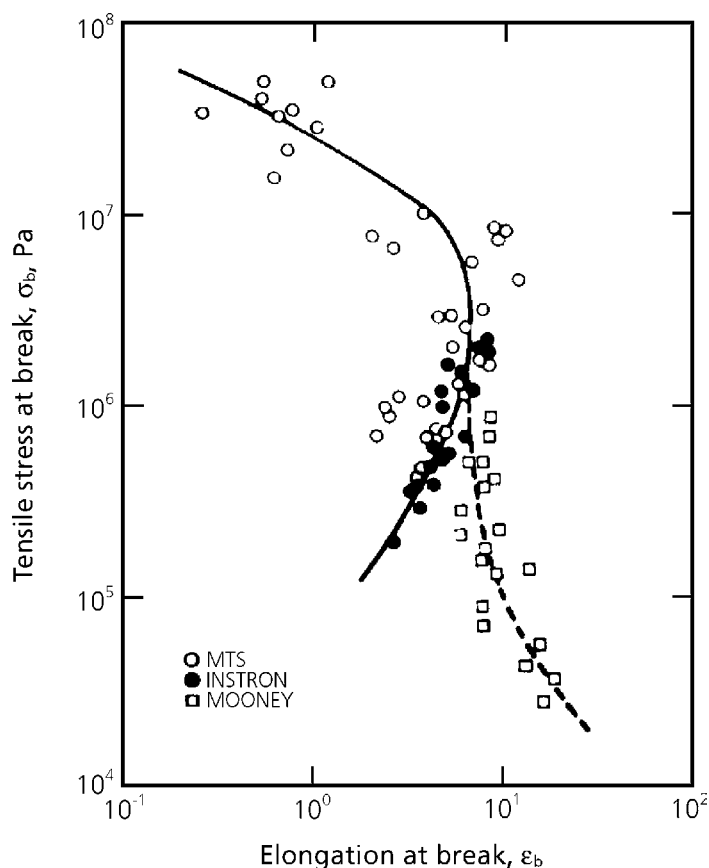


Figure 8.4 Ultimate properties.

Reprinted from N. Nakajima and E. A. Collins, *Rubber Chemistry and Technology*, 1977, 50, 4, 791. Copyright 1977, Rubber Division of the ACS.

The solid curve represents locus of the stress and strain at break, observed with elongation and the broken curve with shear after converting the shear strain to the elongational equivalent. A reasonable agreement between the elongation data and shear data shows that rubber breaks prior to exhibiting a flow-like behaviour. Because the rotational rheometer used has a wide distribution of the strain, the highest strain was used in the above calculation.

A gradual decrease of the torque curve passing the peak in Figure 4.6 indicates that the break is progressing in the rubber contained in the rheometer cavity.

In Figure 8.3, the curves are concave-upward in shape and the trend becomes more prominent at the higher shear rate. In this plot the slope of the curve is the shear stress, τ .

For a constant shear rate, $\dot{\gamma}$, the stress must be constant and independent of L/D. The increasing slope implies that the viscosity increases with L/D.

$$\tau = \eta \dot{\gamma} \quad (8.1)$$

This was previously interpreted as a pressure effect because with the larger L/D, a higher pressure is required to extrude the rubber. However, this interpretation may be incorrect, because gum rubber is practically incompressible and therefore, viscosity is not expected to depend upon pressure. This is demonstrated in the following experiments.

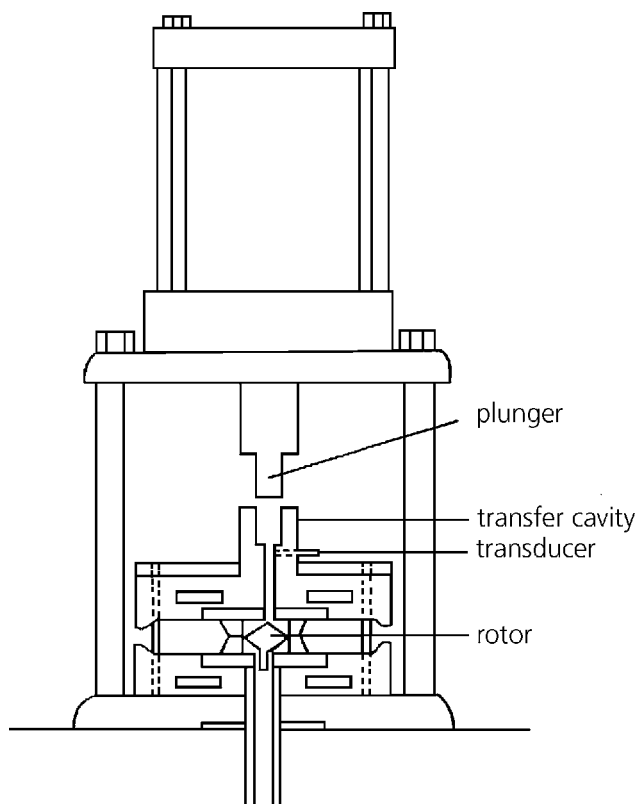


Figure 8.5 Schematic of rebuilt pressurised multispeed viscometer.

Reprinted from S. Montes, J. L. White, N. Nakajima, F. C. Weissert and K. Min, Rubber Chemistry and Technology, 1988, 61, 4, 689. Copyright 1988, Rubber Division of the ACS.

Figure 8.5 shows a rotational rheometer, which is modified to apply static pressure on the sample in the rheometer cavity [4]. This is done by charging an excess sample from the top and pressing it with a plunger. This device enables the maintenance of a constant pressure during the measurement of viscosity. On the other hand with a capillary rheometer the static pressure on the sample is variable, decreasing from the barrel pressure to near ambient pressure at the exit. With this rotational rheometer a number of measurements were made with NR, *cis*-1,4-BR, S-SBR, NBR, EPDM and FPM fluoroelastomer at 44, 60, 80 and 100 °C over the shear rate range of 3×10^{-2} and 2.5 s^{-1} . No perceptible pressure effect was found at the applied pressure of 1.1 and 6.4 MPa. Examples of the pressure effects are shown in Figures 8.6 and 8.7.

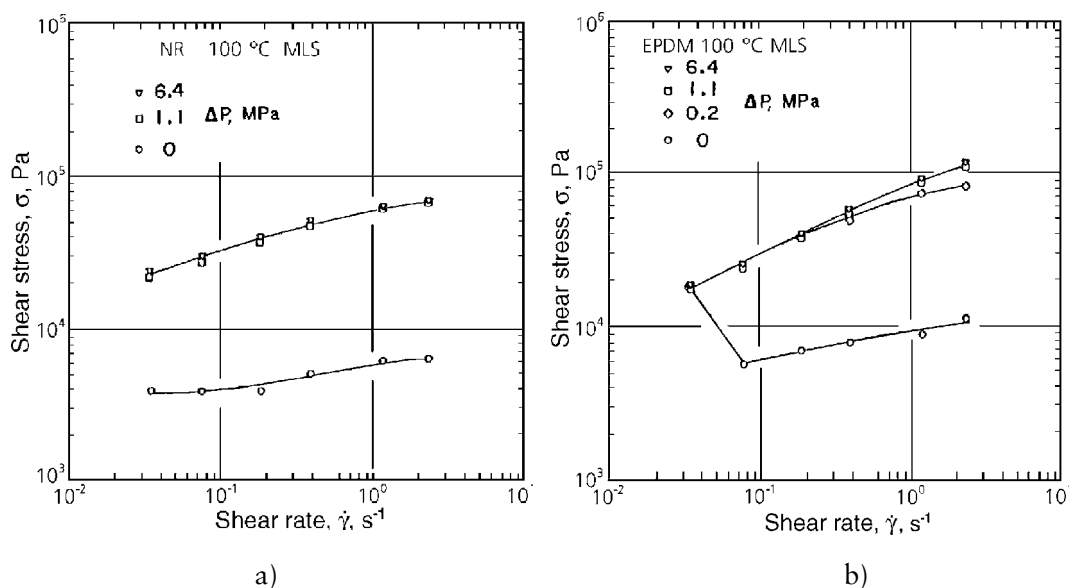


Figure 8.6a Shear stress σ_{12} as a function of shear rate $\dot{\gamma}$ for gum NR (SMR-5) from a Mooney disk rheometer with a smooth rotor. The influence of pressure is shown. $T = 100^\circ\text{C}$.

Figure 8.6b Shear stress σ_{12} as a function of shear rate $\dot{\gamma}$ for gum EPDM from a Mooney disk rheometer with a smooth rotor. The influence of pressure is shown. $T = 100^\circ\text{C}$.

Reprinted from S. Montes, J. L. White, N Nakajima, F. C. Weissert and K. Min, *Rubber Chemistry and Technology*, 1988, 61, 4, 689. Copyright 1988, Rubber Division of the ACS.

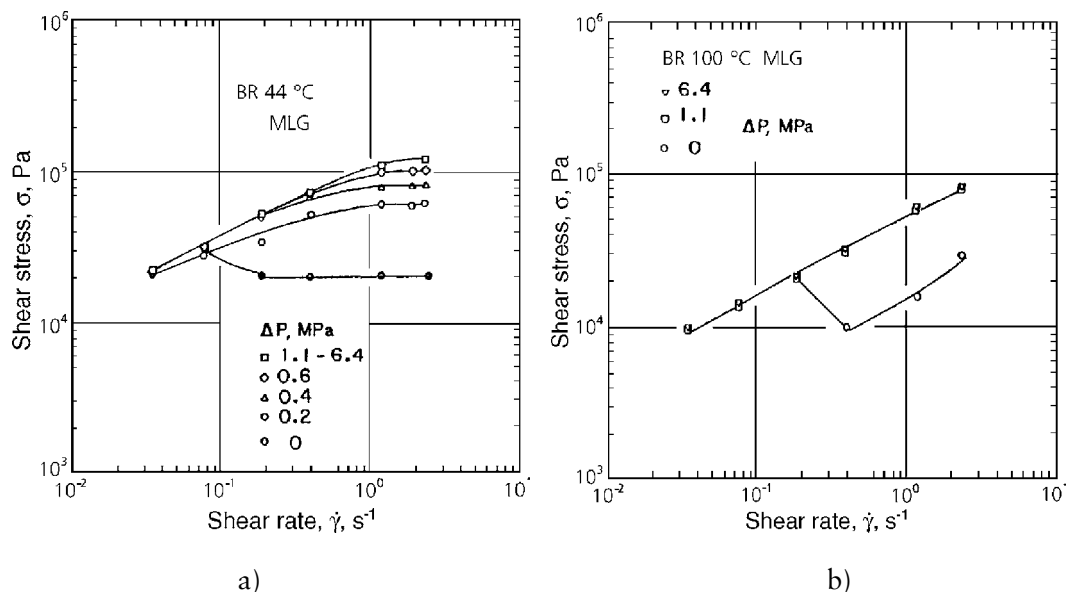


Figure 8.7a Shear stress σ_{12} as a function of shear rate $\dot{\gamma}$ for gum BR from a Mooney disk rheometer with a grounded rotor. The influence of superposed pressure is shown at 44 °C.

Figure 8.7b Shear stress σ_{12} as a function of shear rate $\dot{\gamma}$ for BR from a Mooney disk rheometer with a grounded rotor. The influence of superposed pressure is shown at 100 °C.

Reprinted from S. Montes, J. L. White, N. Nakajima, F. C. Weissert and K. Min, *Rubber Chemistry and Technology*, 1988, 61, 4, 689. Copyright 1988, Rubber Division of the ACS

These results show that the upwardly concave curves of Figure 8.3 are not due to the pressure-effect on viscosity. For some reason a higher pressure is required to extrude gum rubber for a longer L/D. A possible explanation is that the behaviour of gum rubber is not really a flow, a fact which is obvious in the fractured extrudate. The fracture is initiated by a vacuole formation as explained in Chapter 4. The higher pressure suppresses the vacuole formation; therefore, a higher force is necessary for the fracture to occur.

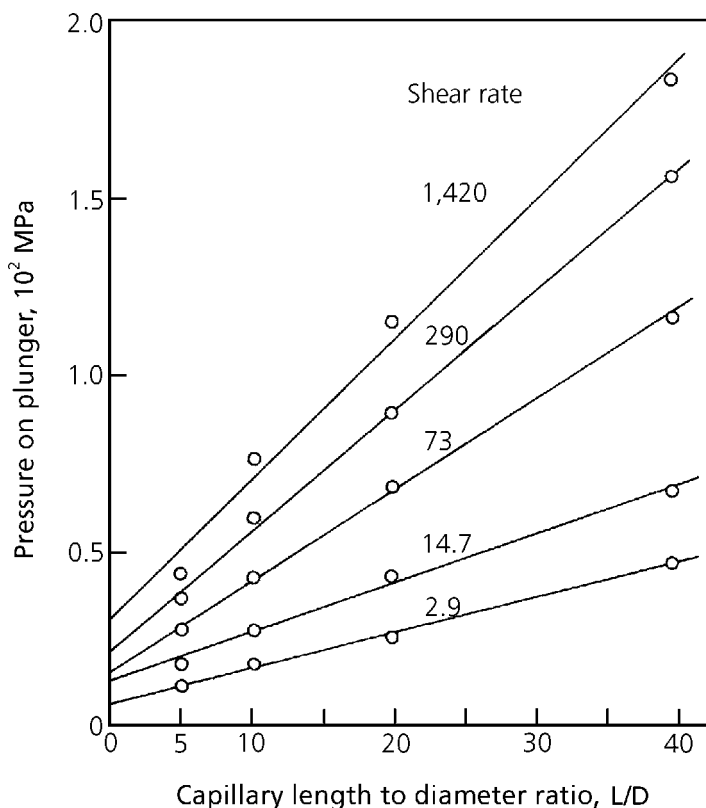


Figure 8.8 Pressure as a function of capillary L/D. Sample 2; shear rates in s⁻¹ as indicated; 125 °C.

Reprinted from N. Nakajima and E. A. Collins, *Rubber Chemistry and Technology*, 1975, 48, 4, 615. Copyright 1975, Rubber Division of the ACS.

Figure 8.8 is a plot similar to Figure 8.3 except that the sample is an NBR compound containing 40 phr of carbon black N550 [5]. The plots are not concave upward. The compound consists of supermolecular flow units, created during mixing. Therefore, it is a flowable material and no fracture is required. In a closer examination these curves may be concave downward. If this trend is real, there are possible explanations; one is a possible inward migration of the filler particles away from the capillary wall. The other is a slip at the capillary wall. Both phenomena may become prominent at the higher shear rate and with the larger L/D.

8.2 Slip

It is obvious that in rubber processing there will be slip, because the surface of processing equipment in contact with gum rubbers and compounds is usually shiny. This is in contrast to plastic processing equipment, in which the surfaces become coated with a thin layer of the degraded material. With plastics this fact indicates the velocity of the melt at the metal interface is zero, i.e., laminar shear flow. A study of slip is multi-faceted, because there are many types of slip, a steady slip, slip with a lubricated layer, slip-stick, slip involving a fracture at the interface or rubbing like a dynamic friction measurement.

In this section slip is treated as if it were one type of behaviour. In Figures 8.6 and 8.7 at the static pressure of 0.6 MPa or lower the shear stresses are considerably lower than the values at 1.1–6.4 MPa. The deviation is larger at the lower pressure and also at the higher shear rate. This indicates the presence of slip. At atmospheric pressure, there is a large reduction of the resistance (expressed as shear stress). However, at very low shear rates, there is no reduction of the resistance, indicating that the sample contact with the rotor is good.

A similar observation is made with carbon-black compounds. Examination of the sheared samples indicated a failure of adhesion of material to the rotor, starting from the location of the highest deformation, i.e., the periphery of the rotor, and progressing inward.

The movement of material in the barrel of a capillary rheometer was used to observe the wall slip [6]. SBR 1500 (E-SBR) and its compounds are used with a flow marker as illustrated in Figure 8.9.

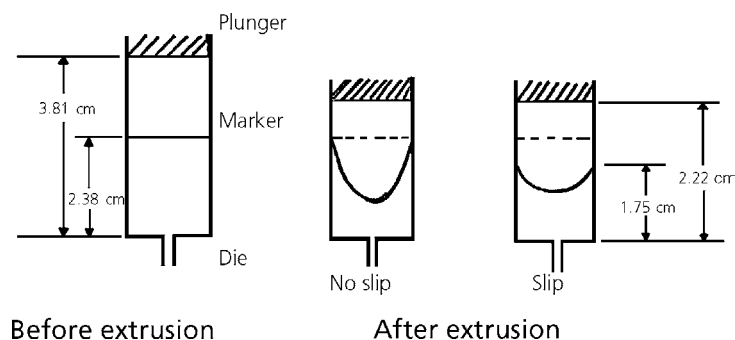


Figure 8.9 Marker technique used for observing wall slippage of elastomer compounds.

Reprinted from C-Y. Ma, J. L. White, F. C. Weissert, A. I. Isayev, N. Nakajima and K. Min, *Rubber Chemistry and Technology*, 1985, 58, 4, 815. Copyright 1985, Rubber Division of the ACS.

In this experiment the gum rubber did not show a slip but the compounds slipped at a higher loading of the filler (20% volume) see Figure 8.10.

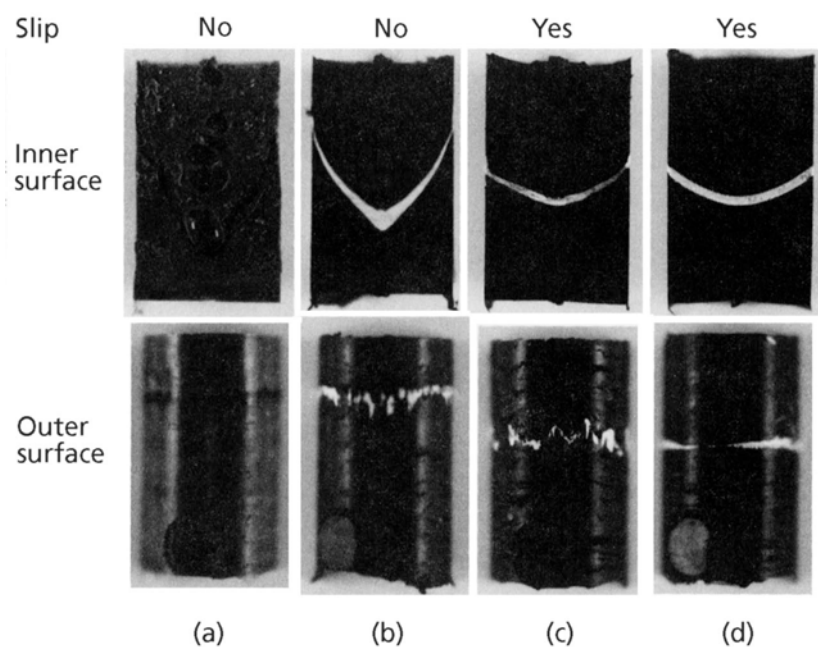


Figure 8.10 Detailed observation of wall slippage for E-SBR and its compounds at 100 °C, $\dot{\gamma}_a = 1.78 \times 10^{-2} \text{ s}^{-1}$.

- a) gum E-SBR
- b) E-SBR + 10 vol% carbon black
- c) E-SBR + 20 vol% carbon black
- d) E-SBR + 30 vol% carbon black

Reprinted from C-Y. Ma, J. L. White, F. C. Weissert, A. I. Isayev, N. Nakajima and K. Min, Rubber Chemistry and Technology, 1985, 58, 4, 815. Copyright 1985, Rubber Division of the ACS.

It showed a slip only at the higher extrusion rate, Figure 8.11.

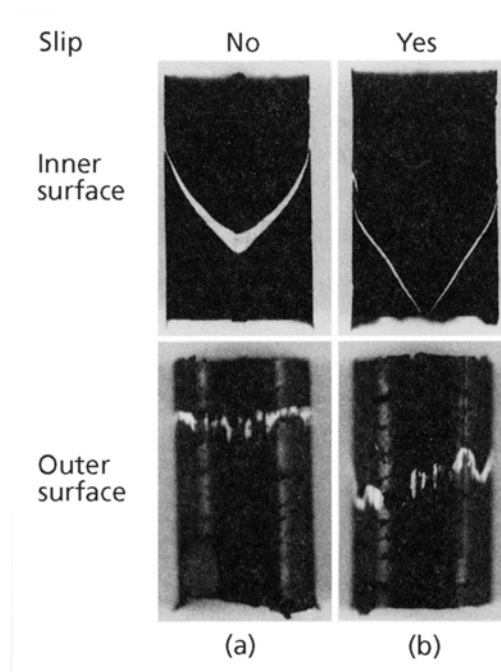


Figure 8.11 Influence of extrusion rate on wall slippage for E-SBR + 10 vol% carbon black at 100 °C.

a) $\dot{\gamma}_a = 1.78 \times 10^{-2} \text{ s}^{-1}$.

b) $\dot{\gamma}_a = 1.78 \times 10^{-1} \text{ s}^{-1}$

Reprinted from C-Y. Ma, J. L. White, F. C. Weissert, A. I. Isayev, N. Nakajima and K. Min, *Rubber Chemistry and Technology*, 1985, 58, 4, 815. Copyright 1985, Rubber Division of the ACS.

8.3 Extrudate shrinkage

Extrudate shrinkage is another way of expressing so-called 'die swell'. In the rubber industry, shrinkage is one of the serious concerns, because the extrudate is cut at a certain length. When there is non-uniform shrinkage, the length of the cut pieces becomes non-reproducible. This causes various problems of material handling. A well-known example is in tyre-building, where the ends of the piece wound around a drum fail to meet.

In this section the phenomenon is described as extrudate swell. Although the practical problem is usually with compounds, the swell of both gum rubbers and compounds will be discussed.

Between gum rubber and compound there are number of differences in the 'extrusion mechanisms'. The gum rubber usually fractures in extrusion but with compounds there is no melt fracture or very slight, when it occurs. The extrudate swell of gum rubber is very large but it is considerably reduced in the presence of filler.

With the plastic melt it was shown that the extrudate swell is a recovery of memory, which was introduced by the deformation of the melt at the entrance to the capillary rheometer. As the melt flows through a capillary, the memory fades by relaxation. Therefore, the shorter the residence time in the capillary, the less memory is lost. This results in the higher swell at the higher shear rate, where the residence time is shorter. Also, the swell decreases with a longer capillary, because the residence time is longer.

Apparently the above interpretation is not applicable to the extrudate swell of gum rubbers. Shown in Figure 8.12 are the shear-rate dependence of swell data of four NBR [1].

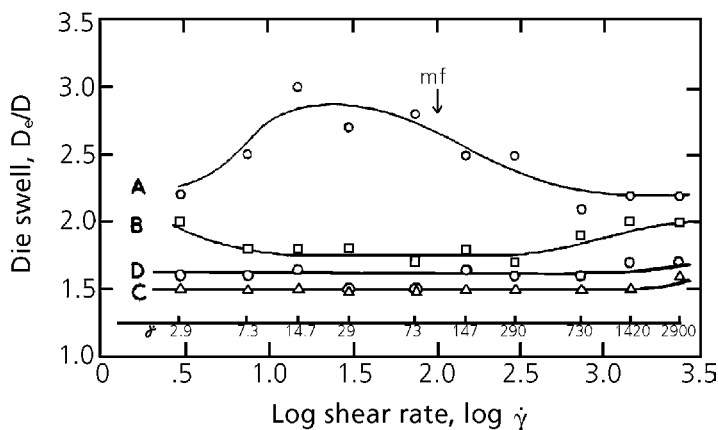


Figure 8.12 Shear rate dependence of die swell at 125 °C, $L/D = 5$ for samples A, B, C and D. See Table 7.2 for description of samples; mf is the onset of melt fracture.

Reprinted from N. Nakajima and E. A. Collins, *Polymer Engineering and Science*, 1974, 14, 2, 137. Copyright 1974, Society of Plastics Engineering.

Only for the lower MW rubber, A, at low shear rate, did the swell increase with increasing shear rate. This shear-rate region of sample A is in the flow state and therefore, the behaviour is similar to that of plastics melt. However, at the higher shear rate, and particularly after the melt fracture the swell decreased significantly. The extrudate going over maximum swell is not generally recognised.

A possible explanation for the decreasing swell with the increasing shear rate is as follows: with the plastic melt and the flow state of rubber, the memory loss results from the relaxation mechanism. In the rubbery state the fracture of the material is involved. The fracture brings about memory-loss also. When the relaxation mechanism contributes less and less and the fracture becomes more dominant, the swell decreases, eventually reaching a constant value.

The decrease of the swell of sample B at the lower shear rate may also be similarly explained. The samples C and D containing a large amount of gel reflect the fracture and consequence of the loss of memory. There is a tendency to increase the swell slightly at the very high shear rate, see Figure 8.12. This behaviour may be attributable to the more elastic nature of the material at the higher shear rate.

The L/D dependence of the swell is shown in Figure 8.13 [1]. The decrease of the swell with the increase of L/D indicates that the relaxation mechanism is also operating with samples A and B. A mechanism of the memory loss with the samples C and D is through fracture.

Figure 8.14 shows the shear rate dependence and L/D dependence of extrudate swell of compound [2]. Both dependencies are there even though they are rather small compared to those of gum rubbers. The trend is to imply a relaxation mechanism, the higher swell at the higher shear rates and the lower swell with the larger L/D. The deformation of the supermolecular flow units and their relaxation may be the explanation.

There is a longstanding question as to whether long branching increases extrudate swell or not. One argument is that it does increase swell. This opinion is based on the observations on melt processing of plastics, for example, film-drawing. When the drawing-speed is increased, the film eventually becomes stiff and difficult to draw. Sometimes, the film vibrates and tears. When long branches are present in the polymer the above behaviour is accentuated. In general, behaviour like this observed in plastic processing is loosely termed 'elastic'. When the behaviour becomes more elastic because of the presence of long branches, elastic memory increases. Therefore, the extrudate swell, being recovery of memory, increases.

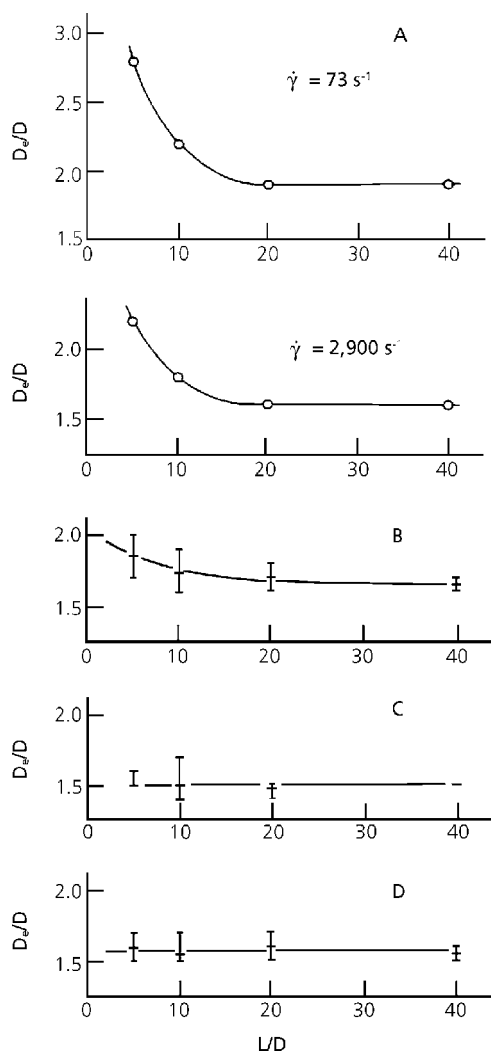


Figure 8.13 Dependence of die swell on capillary L/D at 125 °C for Samples A, B, C, and D. See Table 7.1 for description of samples.

Reprinted from N. Nakajima and E. A. Collins, Polymer Engineering and Science, 1974, 14, 2, 137. Copyright 1974, Society of Plastics Engineering.

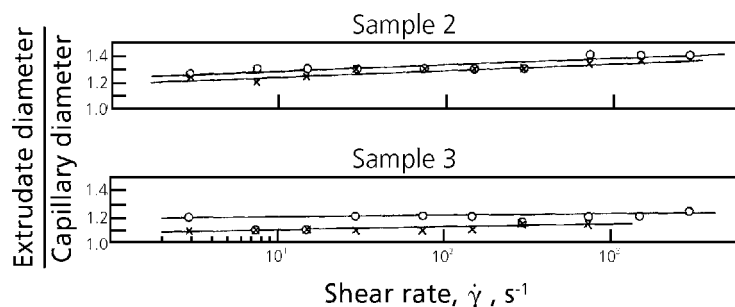


Figure 8.14 Extrudate diameter as a function of shear rate, Samples 2 and 3 of Table 7.1.

L/D = 5 (o); L/D = 40 (x).

Reprinted from N. Nakajima and E. A. Collins, *Rubber Chemistry and Technology*, 1975, 48, 4, 615. Copyright 1975, Rubber Division of the ACS.

The other argument which opposes to the previous argument is based on fundamental viscoelastic studies with ‘monodispersed’ polymers, where the only variable is the long branch, linear versus equal-arm star branch molecule. The steady state compliance of the branched polymer is lower than that of the linear polymer; therefore, the steady state memory in the former is less than that in the latter. This means the extrudate swell of the branched polymer is less than that of the linear polymer.

The error in both arguments is that the variety of branch pattern is not recognised. The error in drawing the conclusion from the fundamental study is that it does not recognise the distinction between linear and nonlinear viscoelastic behaviour. Whereas the fundamental studies are conducted under small deformations where the material behaviour is linear, the extrudate swell concerns nonlinear, large deformation. There is a possibility that the relative degree of swelling between two samples at the small deformation may be reversed at the large deformation. This is one of the ‘crossover’ phenomena.

The crossover may occur also with shear rate such that the relative degree of swell at the lower shear rate may be reversed at the higher shear rate. At the lower shear rate the relaxation of memory is operating but at the higher shear rate the memory loss resulting from fracture may dominate. If the branching introduces long relaxation times, it enhances the swell at the lower shear rate. If the branching results in fracture, the swell is decreased at the higher shear rate. Therefore, whether long branches increase the swell or not depends upon the branch pattern and the extrusion conditions.

This discussion concerns the fully recovered extrudate. In reality the recovery of memory is time-dependent. Cotten conducted a detailed study of the time-dependence with a use of laser beam [7, 8]. SBR 1500 containing 50 phr of carbon black of representative commercial grades was used. A major discovery was the presence of two mechanisms; one was a very fast recovery at less than 0.1 seconds. The other was a much slower recovery towards an equilibrium. The latter is what may be expected from the viscoelastic nature of the material and similar to that observed with plastic melts [9]. The fast recovery had never been observed before, although the die swell of plastic melts had sometimes been arbitrarily classified into a fast and a slow part. The magnitudes of the fast and slow swell were about the same at 25 – 37% at 350 s^{-1} shear rate.

In detail, the fast recovery is clearly related to the surface area and the structure of carbon black, the larger the surface areas by nitrogen absorption (see Chapter 9) and the lower the structure by dibutyl phthalate (DBP) absorption (see Chapter 9) the larger is the swell. The slow recovery was not clearly related to the carbon black properties. What causes the fast and slow recovery is the subject of future study. The fast recovery may primarily be related to the deformation of carbon black network and the slow recovery to the deformation of the rubber matrix.

8.4 Yielding

The yielding of compounds have been observed in elongational as well as in flow measurements. An example of the latter is shown in Figure 8.15 [10].

An extensive examination was conducted on the yielding phenomena associated with various rheological measurements with an NR and S-SBR. Carbon blacks were N110, N326 and N990 at 0, 10, 20 and 30% by volume. Experiments carried out were (i) stress relaxation, (ii) transient and steady state shear flow, (iii) stress relaxation after steady flow, (iv) sequential shear flow history and (v) storage effect.

The yielding was observed in all these measurements with N110 and N326 at the volume concentration of 20% and higher. This implies the presence of structure built by carbon black. The yield value was significantly dependent on the previous shear history; the milder the shear treatment the larger was the yield value, as shown in Figure 8.16, of the relaxation curves and in Figure 8.17 of relaxation after cessation of flow. Destruction of the structure occurs to a different degree depending upon the severity of the shear history.

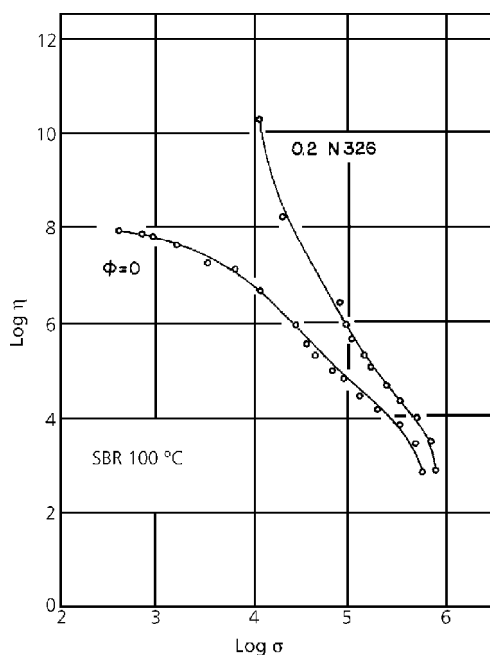


Figure 8.15 Steady state shear viscosity η as a function of shear stress for SBR and its 0.2 phr N326 carbon black compounds, $T = 100\text{ }^{\circ}\text{C}$.

Reprinted from S. Montes, J. L. White and N. Nakajima, *Journal of Non-Newtonian Fluid Mechanics*, 1988, 28, 183. Copyright 1988, with permission from Elsevier Science.

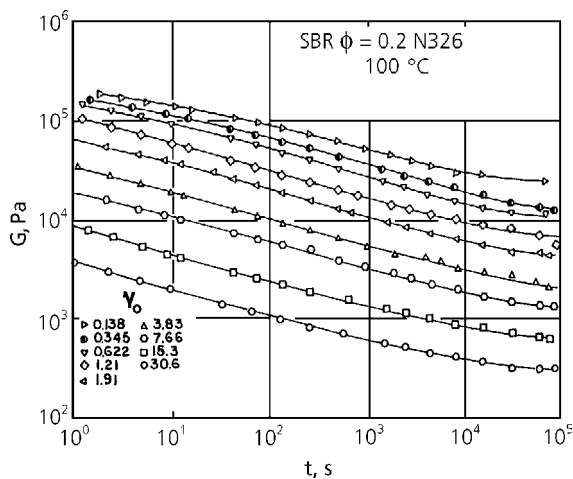


Figure 8.16 Relaxation modulus $G(t)$ from small instantaneous strains. SBR + 0.2 phr volume fraction black, $T = 100\text{ }^{\circ}\text{C}$.

Reprinted from S. Montes, J. L. White and N. Nakajima, *Journal of Non-Newtonian Fluid Mechanics*, 1988, 28, 183, Copyright 1988, with permission from Elsevier Science.

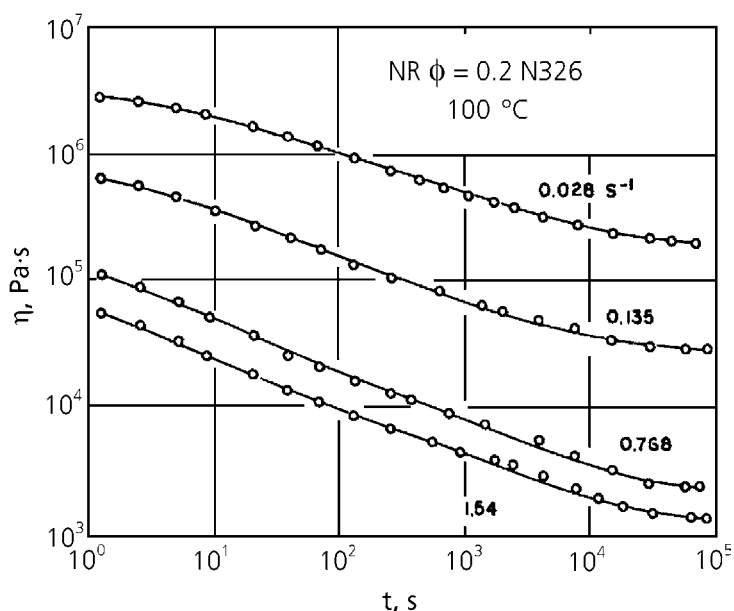


Figure 8.17 Shear viscosity relaxation following flow for NR + 0.2 phr N236 black, $T = 100^\circ\text{C}$.

Reprinted from S. Montes, J. L. White and N. Nakajima, *Journal of Non-Newtonian Fluid Mechanics*, 1988, 28, 183, Copyright 1988, with permission from Elsevier Science.

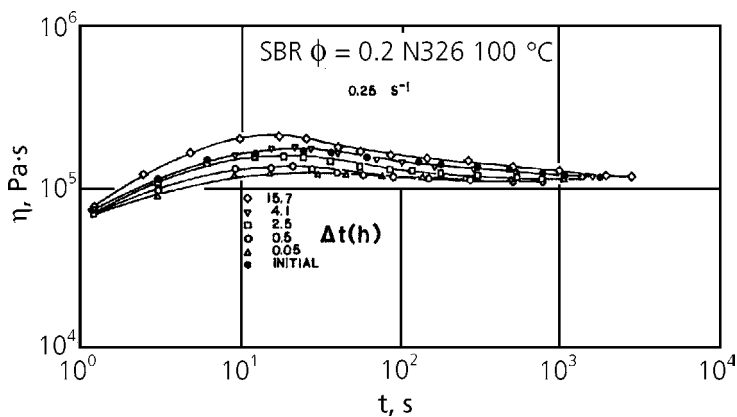


Figure 8.18 Sequential transient shear viscosity after various periods of rest for SBR. SBR + 0.2 phr N236 black, $T = 100^\circ\text{C}$.

Reprinted from S. Montes, J. L. White and N. Nakajima, *Journal of Non-Newtonian Fluid Mechanics*, 1988, 28, 183, Copyright 1988, with permission from Elsevier Science.

With storage, the modulus and yield value recover to the original values and eventually even surpass them.

Recognising that the original sample had some prior shear treatment, such as charging into the rheometer or even history of mixing, the recovery surpassing the original value is not surprising.

What we learn from the yielding study is that the mutual arrangement of carbon black aggregates, sometimes called ‘carbon black network’, takes a variety of forms, which are quasi-stable. It changes slowly with time towards a more stable form. Because diffusion of carbon black particles is negligible, the driving force of the aggregate-structure change must come from viscoelastic memory of the compound. The detail of this mechanism will be the subject of future study.

8.5 Effect of concentration and structure of carbon black

8.5.1 Hydrodynamic theories

The starting point for discussion is an idea that the modulus, E of the filled rubber is related to the modulus, E_0 , of the unfilled counterpart:

$$E = f(v) E_0 \quad (8.2)$$

Where $f(v)$ is a function relating these two moduli which is dependent on the volume fraction, v , of the filler. This relationship is sometimes given in the following form,

$$E = E_0(1 + c_1v + c_2v^2) \quad (8.3)$$

where

$$f(v) = 1 + c_1v + c_2v^2 \quad (8.4)$$

Physical explanation of this expression is usually given in steps. Smallwood [11] derived a theoretical expression for modulus increase by the presence of an isolated, rigid sphere. Complete adhesion of the rubber matrix on the surface of the sphere is assumed. For a small deformation, i.e., extrapolated to zero elongation, it gives an expression:

$$E = E_0 (1 + 2.5v) \quad (8.5)$$

Smallwood noted the similarity of this equation to Einstein’s viscosity equation [12]

$$\eta = \eta_0 (1 + 2.5v) \quad (8.6)$$

where η and η_0 are the viscosity of suspension and that of the medium, respectively.

Subsequently, Guth and Gold [13], considering the interaction of a pair of spheres embedded in a moving fluid, added the higher term in the concentration dependence as,

$$\eta = \eta_0 (1 + 2.5\nu + 14.1 \nu^2) \quad (8.7)$$

In recognising a similarity between Equations 8.5 and 8.6, Guth [14] adopted Equation 8.7 for the modulus of rubber containing a pair of interaction spheres.

$$E = E_0 (1 + 2.5\nu + 14.1 \nu^2) \quad (8.8)$$

This equation is still for a low concentration of the filler, where only binary interaction is considered. The Equations 8.5 and 8.8 are sometimes called hydrodynamic theories [15]. For a yet higher concentration Guth produced a model that showed that the filler particles line up in a straight line forming a rod-like chain. For this rod a shape factor, f , is assigned, representing the length to breadth ratio. With this rod-model, Guth [14] considered inter-rod binary interaction and derived the following expression,

$$E = E_0 (1 + 0.67 f\nu + 1.62 f^2\nu^2) \quad (8.9)$$

where $f \gg 1$. The shape-factor was interpreted later to represent the anisotropic shape of the single filler particle as rod-like [15].

Considering a highly irregular shape and a presence of 'occluded rubber' in cavities of the carbon black aggregates, Medalia [16] introduced 'effective volume' to represent filler concentration. His effective volume fraction, V , replaces the real volume fraction, ν , in Equation 8.8. The effective volume fraction, V , is not an adjustable parameter, but calculated from the DBP absorption [17] (see also Chapter 9). The shear storage modulus, G' , was measured at 25 °C and 0.25 Hz, with 20 phr of carbon black loading where G' was practically independent of the strain amplitude. With 12 carbon blacks of varying particle size and structure, the calculated, G' , from the equation,

$$G' = G'_0 (1 + 2.5V + 14.1 V^2) \quad (8.10)$$

were in agreement with observed values to within 5%.

Recalling the assumptions involved in deriving Equation (8.8), it may be concluded that when the occluded volume correction is made as suggested by Medalia [16], the sphere model for an isolated filler particle is a good approximation; this conclusion is valid only at a low loading, where the modulus is practically independent of strain amplitude, and only binary interaction between particles needs to be considered.

For a higher loading where the modulus decreases [18] with the increasing strain amplitude, Medalia [16] took the G' values at 10% strain amplitude. At this point the modulus has decreased significantly, presumably as a result of breaking the carbon black network. The calculated G' were in good agreement with the observed ones within 10% for the same 12 carbon blacks.

Medalia [16] demonstrated a further usefulness of this approach by using graphitised carbon blacks, which are known to have a weaker surface-affinity towards rubber. Thus, the method provides a means of examining the filler-rubber interaction. However, by the conditions set for deriving Equation 8.10, its applicability is limited to a small deformation. Also, only bi-particle interactions are considered in the equation and multi-particle interactions are assumed to be negligible. For the filled-rubber with the normal loading of 40-50 phr, the carbon black particles are crowded and the multi-particle interaction is important.

Because of the assumption involved in deriving Equations 8.7 and 8.8, the above correlations should be regarded as an empirical nature. With this and with consideration of the dependence of the viscoelastic properties on the time scale, the quantitative relationship of the viscoelastic properties to the concentration and properties of the carbon black must be examined case-by-case.

8.5.2 Concentration dependence

In general the concentration dependence of viscosity of dispersed spheres may be described with a form of equation given by Eilers [19].

$$\eta_r = \left[1 + \frac{2.5\nu}{2\left(1 - \frac{\nu}{b}\right)} \right]^2 \quad (8.11)$$

when η_r is the ratio of the viscosity of the dispersion to that of the medium and b is a constant determined by the mode of packing of spheres. For infinite dilution, Equation 8.11 is reduced to Einstein's equation, Equation 8.6. As the concentration is increased, the viscosity increases rapidly towards infinity when ν approaches b . At $\nu = b$, the tight packing of spheres presumably prevents flow. A more general form of Eiler's equation is given by Maron and Belner [20] as

$$\eta_r = \left[1 + \frac{\alpha v}{1 - \beta v} \right]^2 \quad (8.12)$$

where α and β are constants determined by the nature of the dispersion.

Many equations similar to Eilers' equation have been proposed; for example, Maron's [21] equation is,

$$\eta_r = \frac{(\epsilon v)^m}{(1 - \epsilon v)^n} \quad (8.13)$$

where ϵ , m , and n are material constants; the exponent, m , may be zero or positive and n is a positive non-zero number. There are many variations of these equations, which reduce to the identical forms at the infinite dilution and at the highest allowable concentration at the tight packing. Therefore, the variation of the forms concerns the concentration dependence between the two limits.

In applying these equations other important considerations, namely the non-Newtonian nature of the flow also needs to be considered. A similar form of equation may be used to represent the modulus of the dispersed systems. However, for the modulus both strain- and strain-rate dependence must be considered.

References

1. N. Nakajima and E. A. Collins, *Polymer Engineering and Science*, 1974, **14**, 2, 137.
2. N. Nakajima and E. A. Collins, *Rubber Chemistry and Technology*, 1974, **47**, 2, 333.
3. N. Nakajima and E. A. Collins, *Rubber Chemistry and Technology*, 1977, **50**, 4, 791.
4. S. Montes, J. L. White, N. Nakajima, F. C. Weissert and K. Min, *Rubber Chemistry and Technology*, 1988, **61**, 4, 698.
5. N. Nakajima and E.A. Collins, *Rubber Chemistry and Technology*, 1975, **48**, 615.

6. C-Y. Ma, J. L. White, F. C. Weissert, A. I. Isayev, N. Nakajima and K. Min, *Rubber Chemistry and Technology*, 1985, **58**, 4, 815.
7. G. R. Cotten, *Rubber Chemistry and Technology*, 1979, **52**, 1, 187.
8. G. R. Cotten, *Rubber Chemistry and Technology*, 1979, **52**, 1, 199.
9. N. Nakajima and M. Shida, *Transactions of the Society of Rheology*, 1966, **10**, 299.
10. S. Montes, J. L. White and N. Nakajima, *Journal of Non-Newtonian Fluid Mechanics*, 1988, **28**, 183.
11. H. M. Smallwood, *Journal of Applied Physics*, 1944, **15**, 11, 758.
12. A. Einstein, *Annals of Physik*, 1906, **19**, 289.
13. E. Guth and O. Gold, *Physics Review*, 1938, **53**, 322.
14. E. Guth, *Journal of Applied Physics*, 1945, **16**, 1, 20.
15. E. M. Dannenberg, *Rubber Chemistry and Technology*, 1975, **48**, 3, 410.
16. A. I. Medalia, *Rubber Chemistry and Technology*, 1973, **46**, 4, 877.
17. ASTM D 2414-99
Standard Test Method for Carbon Black-n-Dibutyl Phthalate Absorption Number.
18. A. R. Payne, *Journal of Applied Polymer Science*, 1962, **6**, 19, 57.
19. H. Eilers, *Kolloidnyi Zhurnal*, 1941, **97**, 313.
20. S. H. Maron and R. J. Belner, *Journal of Colloid Science*, 1955, **10**, 6, 523.
21. S. H. Maron and P. E. Pierce, *Journal of Colloid Science*, 1956, **11**, 1, 80.